EXPERIMENTAL STUDY OF RIVULET LIQUID FLOW ON AN INCLINED PLATE

Adel Ataki and Hans-Jörg Bart

Universität Kaiserslautern, Lehrstuhl für Thermische Verfahrenstechnik
D - 67663 Kaiserslautern, Germany

http://www.uni-kl.de/LS-Bart/

Abstract

Many chemical processing applications involve liquid film flow in a form of rivulets on an inclined plate, such as the flow on an element of structured packings which consists of a number of metal lamellas in a certain geometry. A better understanding of this kind of flow would provide a help to further develop the structure of such packings and to get a better performance under the same conditions and available work space. Experimental data of a water-glycerine mixture are compared with the models from literature and with CFD simulations using the VOF (Volume of Fluid) model, which is implemented in the commercial software FLUENT®. The contact angle was measured using an optical method with a CCD camera. For the determination of the film height and rivulet width an optically assisted sensor was constructed, which can be applied with complex structured geometries. The effect of the mean velocity and contact angle on the rivulet profile will be discussed.

Introduction

Rivulet flow is a special case of film flow when the flow rate is small enough that the film develops to a trickle with a specific profile [1]. Such kind of flow can be found in the process engineering applications such as the flow in a trickle reactor and structured packed columns used for evaporation and distillation. A better understanding of the hydrodynamics of rivulet flow allows to develop optimal packing structures in respect to mass transfer and hydrodynamics.

The scope of this paper is to describe the rivulet flow on a plain inclined plate and compare the experimental results with models from literature [2, 11] and CFD calculations. This should serve as a basis when considering more complex geometries. A major problem in respect to that is a precise film thickness analysis. Methods discussed in literature [3, 4, 8, 9, 10] needs calibration when reflecting a fluorescence signal on a black background [3, 4] or transmitting signals through glass [8, 9, 10] and can thus not be directly used with an inclined metal plate or structured packing element. An optically assisted sensor system has been developed to determine the spatial thickness of the film at any point of the rivulet with an error less than 10 µm as outlined below.

Theory

To describe the rivulet flow it is necessary to describe the interfacial profile and the local velocity distribution. A set of appropriate assumptions which simplify the general Navier–Stokes equations are as follows:

- the flow is one dimensional and parallel to x axis (u = v = 0),
- there is fully developed flow, that means uniform rivulet width and the height is constant in the direction of flow,
- the liquid is incompressible,
- there is no shear stress at the gas-liquid interface, and
- there are steady state condition.

Equations (1-3) are the reduced form of Navier-Stokes equations were z is the flow direction as shown in Fig.(1):

$$\frac{\partial p}{\partial x} = 0 \tag{1}$$

$$\frac{\partial p}{\partial y} = -\rho.g.\sin\alpha \tag{2}$$

$$\frac{\partial^2 w}{\partial x^2} + \frac{\partial^2 w}{\partial y^2} = -\frac{g.\cos\alpha}{\nu} \tag{3}$$

The pressure is constant along the x-axis (s. equ. (1)) and the hydrostatic pressure gradient along the y axis is given with equ. (2). The velocity distribution and rivulet profile is given by equ. (3), which balances viscous and gravitational forces.

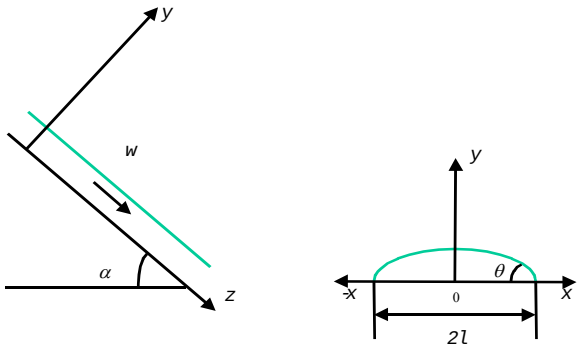

Fig. 1 Rivulet flow parameters
α:Inclination of plate, θ::contact angle at the side of the rivulet, 2l:width of the rivulet

To solve the momentum equ. (3) the interfacial profile and velocity distribution need to be known. Duffy et al. [2] have given an approximated solution for equ. (3) using the expression for the curved interface (4):

$$p(\eta) = p_g - \frac{\gamma.\eta''}{(1+\eta'^2)^{3/2}} \tag{4}$$

where $\eta(x)=y(x)$, η', η'' are the first and second derivatives with respect to *x* and γ is the surface tension.

Here the velocity profile is only function of y:

$$\frac{\partial w}{\partial x} << \frac{\partial w}{\partial y} \tag{5}$$

and

$$\eta'^2 << 1 \tag{6}$$

Their solution for the rivulet profile when $\alpha<\pi/2$ is given in equ. (7):

$$\eta(x) = (\frac{\gamma}{\rho g\,|\sin(\alpha)|})^{1/2} \tan\theta \frac{\cosh B - \cosh \zeta B}{\sinh B} \tag{7}$$

where $\zeta=y/l$, l is the half rivulet width, ρ is density, μ is viscosity and B is Bond number as to

$$B = l(\frac{\rho.g.|\cos(\alpha)|}{2.\mu}) \tag{8}$$

Towell et al. [11] have also given approximated solutions for the three cases of flat ($a/b<<Y$), small ($a/b>>Y$), and the general rivulet flows. However the curved interface model according to equ. (4) is also used where the pressure at the interface is set equal to the normal stress and the z stress component equal to zero. The resulting differential equation for the interface is given in the non dimensional form in equ. (9):

$$\frac{Y''}{(1+Y'^2)^{3/2}} = \frac{a}{b} + Y \tag{9}$$

were $a = \sqrt{\gamma / \rho g \sin(\alpha)}$ and $Y = \frac{\eta_0 - \eta}{a}$, $\eta_0 = \eta$ at $x = 0$, $Y=Y(X)$, $X=x/a$, and b is the radius of the interface curvature at $Y=0$.

Equ. (9) represents a family of curves with $a/b=\delta$ as a parameter and only one of them at a definite value of δ describes the interface for a given stream width (or flow rate) and contact angle. To find the interface profile for a given flow rate equ. (9) must be solved together with a flow rate equation which needs a velocity profile and interface profile according to equ. (10). This problem has to be solved by iteration using an approximated velocity profile equ. (11) resulted from an approximated non dimensional form of equ. (3) according to equ.(5) as a start point of the solution.

$$Q = \int_{-l/2}^{l/2} \int_0^{\eta} w(x,y)\,dx\,dy \tag{10}$$

$$w = (Y_0 - Y)\xi - \frac{1}{2}\xi^2 \tag{11}$$

where $\xi=y/a$.

The general solutions of equation (9) are given implicitly by equs. (12) and (13) in respect to the parameter ϕ. This parameter changes from $\pi/2$ at $X=0$ to a minimum value at ϕ_{min} at the other outer edge of the rivulet and can be estimated from the contact angle θ with the equ.(14).

$$X = \frac{2-k^2}{k}[K - F(k,\phi)] - \frac{2}{k}[E - E(k,\phi)] \tag{12}$$

$$Z = \frac{2}{k}\sqrt{1 - k^2.\sin^2\phi} \tag{13}$$

$$\sin(\phi_{\min}) = \cos(\theta/2) \tag{14}$$

where

$$Z = Y + \delta \tag{15}$$

$$k = \frac{2}{\sqrt{4+\delta^2}} \tag{16}$$

and $E(k, \phi)$, $F(k,\phi)$ are elliptical integrals and $E = E(k, \phi_{min})$, $F = F(k,\phi_{min})$ [2].

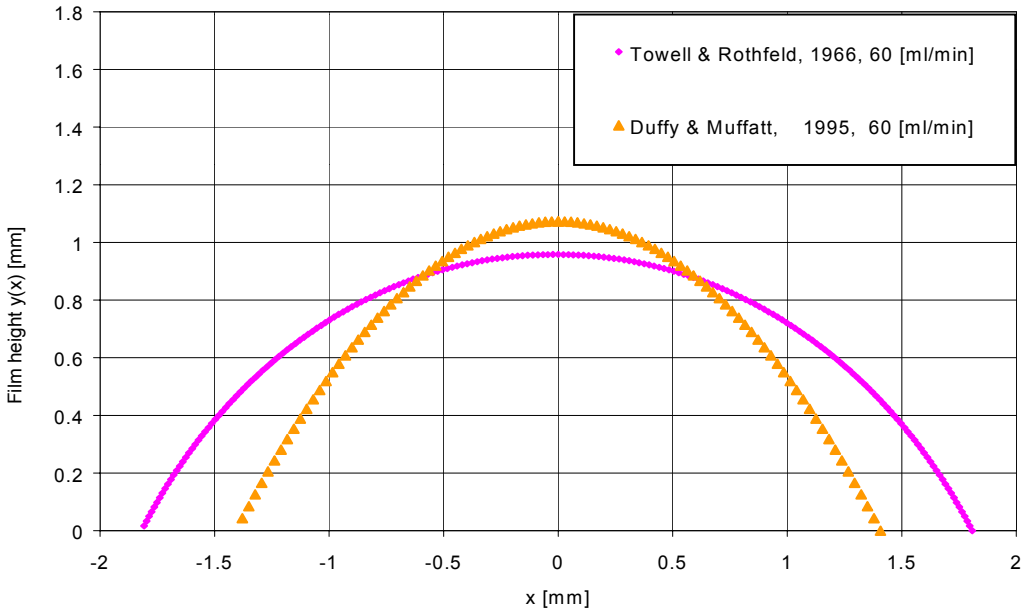

Fig. 2: Rivulet profile of glycerin-water 50% for a flow rate of 60 ml/min and contact angle of 56 degree calculated by the two models

Fig. 2 depicts the rivulet profiles resulted from the two models for the same liquid and contact angle. Towell & Rothfeld [11] predict, as it is seen in Fig. 2, a wider and lower meniscus than that of Duffy & Muffatt [2] with a generally more flat profile for same flow rate. In order to overcome this discrepancy a comparison with CFD simulations with a commercial software FLUENT® using the VOF (Volume of Fluid) model and with experimental data will be given.

CFD simulation

To simulate this kind of flow we used the VOF (Volume of Fluid) model implemented in the FLUENT® code. The VOF is a popular interface tracking algorithm and it is suitable for stratified and free surface flows [5, 13]. It relies on the fact that two or more fluids (phases) are not interpenetrating. Tracking the volume fraction of each fluid throughout the domain follows by solving a continuity equation for the volume fraction of one (or more) of the phases in each cell . For the q_{th} phase, this equation has the form given in the equ. (17):

$$\frac{\partial \varepsilon_q}{\partial t} + \vec{v}.\nabla \varepsilon_q = \frac{S_{\varepsilon_q}}{\rho_q} \tag{17}$$

where ε_q is the volume fraction of the *q*th phase with:

ε_q=0: if cell is empty (of the *q*th phase.)

ε_q=1: if cell is full (of the *q*th fluid)

0<ε_q<1: if cell contains the interface between the *q*th fluid.

By default, S_{ε_q} , is the mass source term for each phase and set equal to zero in absence of the mass transfer between the phases. The volume fraction equation will be computed based on the following:

$$\sum_{q=1}^{n} \varepsilon_q = 1 \tag{18}$$

The properties appearing in the transport equations are determined by presence of the component phases in each control volume. For a two phase flow the density is calculated as follow:

$$\rho = \varepsilon_2 \rho_2 + (1 - \varepsilon_2)\rho_1 \tag{19}$$

All other properties are calculated in the same manner. In this model a single momentum equation is solved throughout the domain, and the resulting velocity field is shared among the phases. The momentum equation is dependent on the volume fractions of all phases through the properties ρ and μ and has the form:

$$\frac{\partial}{\partial t}(\rho\vec{v}) + \nabla.(\rho\vec{v}\vec{v}) = -\nabla p + \nabla.[\mu(\nabla\vec{v} + \nabla\vec{v}^T)] + \rho\vec{g} + \vec{F} \tag{20}$$

The pressure drop accross the interface is calculated according to the folowing equation:

$$p_2 - p_1 = \gamma\left(\frac{1}{R1} + \frac{1}{R2}\right) \tag{21}$$

where p1, p2 are the pressures in the two fluids on each side of the interface. R1, R2 are the radii of the interface curvature. Liquid adhesion to a surface can be set by giving a value for the contact angle from experiments as input data.

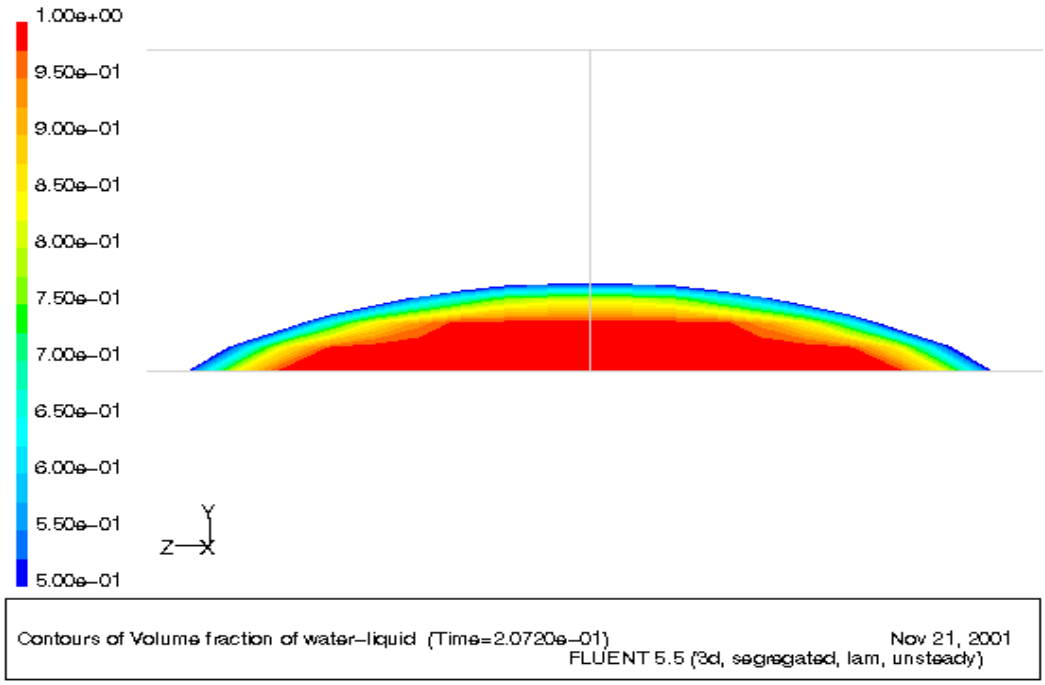

Fig. 3: Rivulet profile from CFD simulation using the VOF model (glycerin-water 50% per weight, 298 K)

For the 3D CFD simulations an inclined plate of 8x2x40 mm dimensions with 19860 hexahedral mesh elements was implemented in the FLUENT@ VOF code. The mesh elements were 0.167 mm in height, 0.25 mm width and 1 mm in length in flow direction. The velocity inlet was chosen as zero pressure inlet and symmetry conditions in respect to the middle of the plate were chosen. The plate had an inclination of α=21.5 degrees. A variation of grid size did not affect the solution but the time steps had to be varied from 10^{-5} s to 10^{-4} s to obtain convergence.
Fig. 3 shows the VOF contour on a plane perpendicular to the plate at a distance of 20 mm from the inlet. The interface was determined at the nodes where VOF is equal to 0.5. All other parameters such as mean velocity and cross section area can be calculated and compared with the experimental and models results.

Experimental results and measuring method
To get a laminar flow with constant flow rate the set up shown in fig. 4 was used. The liquid is pumped (2) from the reservoir (1) to a constant level tank (3) than flows down under the gravity forces through a flow meter (4) to a damping box (5) and a small tube or capillary (6) on the top of a 0.1 mm thickness, 20 mm width and 300 mm long metal sheet (7) inclined with an angle of α= 21.5 degrees. The liquid flows back form the sump tank (8) to the reservoir.

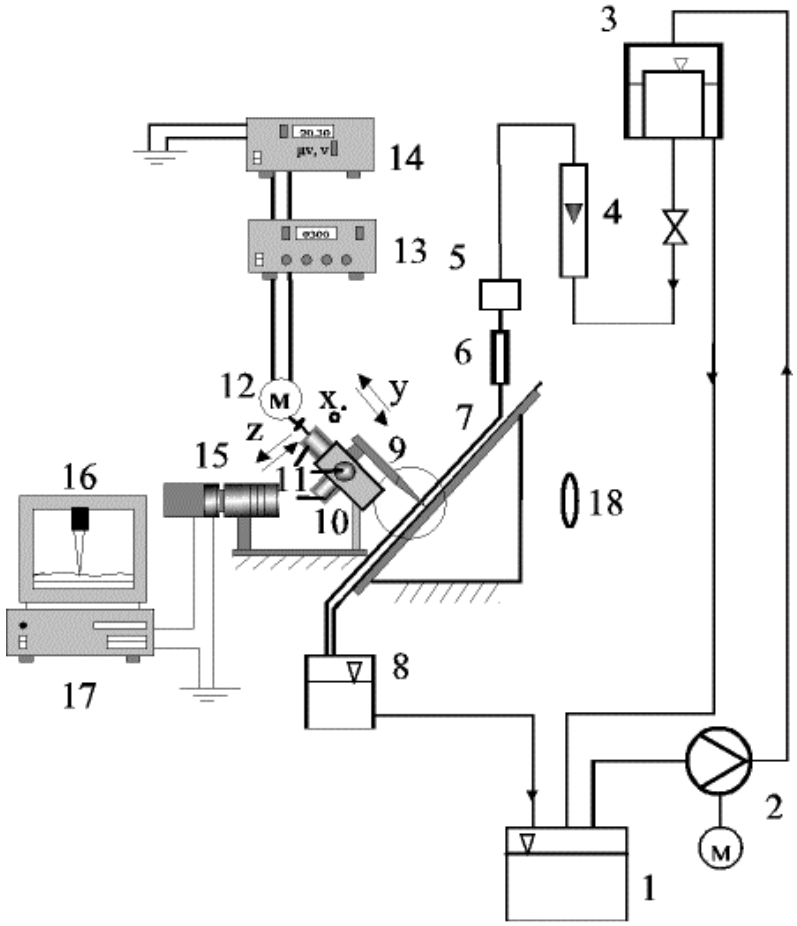

1. Reservoir
2. Circulation pump
3. Constant level tank
4. Flow meter
5. Turbulence damping box
6. Capillary tube
7. Metal sheet
8. Liquid sump
9. Sensor (needle)
10 Moving table
11 Micrometers
12. Step motor
13. Step motor control panel
14 Electrical stabilizer
15 CCD camera
16 Monitor
17 Frame grabber
18 Light source

Fig. 4: Film height measuring apparatus

In order to measure the rivulet height, a simple and direct measuring method with an optically assisted sensor system is used. The sensor consists of a needle with a sharp tip (9) fixed on a movable table (10). This table with the needle can be moved using three micrometer screws (11) in the three directions x, y and z in the space.

One of them is adjusted by an electrical step motor (12) (one step S=5.20833 μm) using a control panel (13). The movements of the needle are viewed on a monitor (16) using a CCD camera (15) equipped with an objective with a zoom factor of 40 and a frame grabber card (17) and a light source (18).
The thickness can then be determined as follows: before the start of measurement the needle tip head position is adjusted to be in an equal distance from the plate along x and z direction using the three micrometers (11) (s. Fig. (5)).First the needle is positioned on a calibrated height n1.S and then the rivulet flows the needle is positioned to n2.S. The local rivulet height is:

$$y(x) = (n1 - n2)S \tag{22}$$

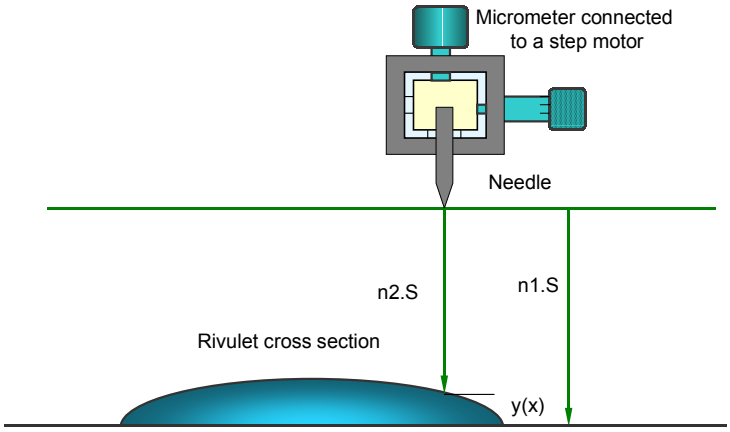

Fig. 5: Film height measurement prenciple

This process is repeated for other locations along the rivulet width from x=0 to 2l. The measuring error using this method is about 10 µm or 2 steps. To measure the film thickness in another location the third micrometer (11) can be used to shift the needle to the new location along z axis.

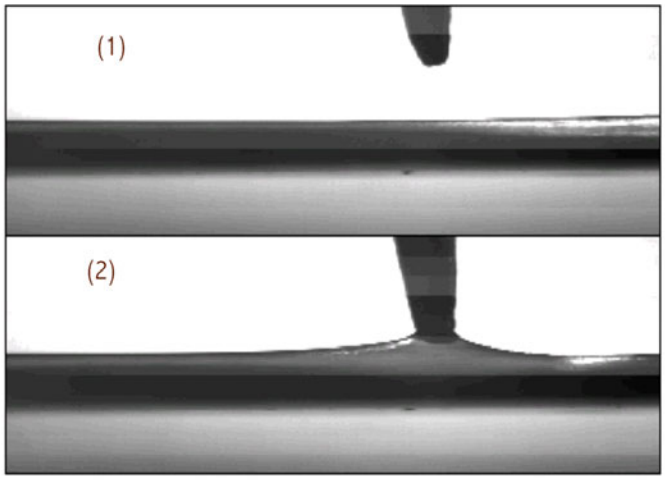

Fig. 6: Liquid attraction to the needle due adhesion forces

Fig. 6 shows a two snap shooting of the needle in a distance to the surface of one step (5.20833 μm). The location of measurement was chosen where the rivulet is uniform and its edges were straight and parallel to each other and to the plate edge. A glycerin-water mixture of 50% per weight was used in the experiments with a density of 1125 kg/m3, a viscosity of 0.004862 kg/m.s and a surface tension of 0.0662 N/m

Fig. 7 shows a set of measurements for different flow rates. From this one can determine the dynamic contact angle at the edge of the rivulet by deriving the extrapolated function at x where $y(x)=0$. The static contact angle measurements have given a value of 56 degrees which differs from the estimated dynamic contact angle of 41.7 degrees. The latter is derived from Fig. 7. The mean velocity can be easily calculated from the cross sectional area derived from the rivulet profile and flow rate.

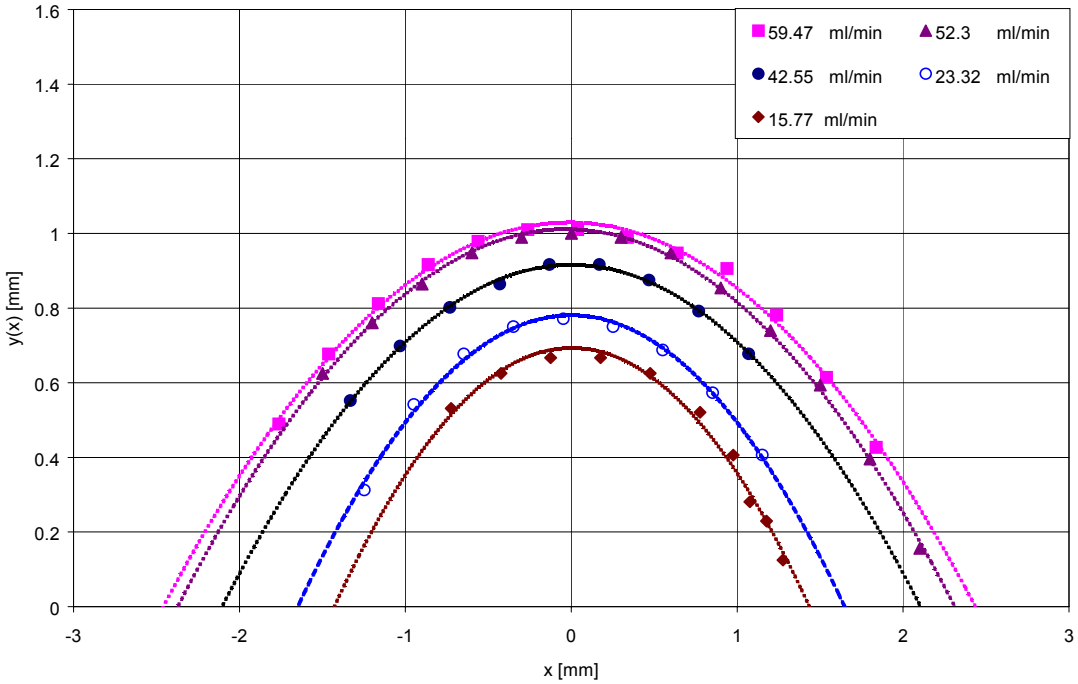

Fig. 7: Experimental results for glycerin-water 50% weight, (298 K)

Some difficulties when applying this experimental method is the measurement of the height of the rivulet near its border especially when the amount of the liquid is small. Here attractive forces of the needle disturb the local flow. However these difficulty can be limited by using a sharper needle. To eliminate the effect of pre-wetting and hysteresis effects due to surface contamination [7] the plate was cleaned for each individual run with distilled water and acetone before air drying.

Results

Figs. 8 and 9 show the rivulet profile calculated by the two models [2, 11] and CFD simulation using the static contact angle value and the experimental results for the above glycerine-water mixture with a flow rate of 15.77 and 39.17 ml/min respectively. The CFD simulation and Towell model [11] are in a very good agreement with the experimental results with a maximum error of about 8 % Duffy model does not represents this flow. Figs. 10 and 11 show the rivulet profile change when using the dynamic contact angle for the same liquid mixture and flow rates. As

can be seen, the Duffy model gives a better approach but the dynamic contact angle should be the outcome of the calculations and not an input from experiments.

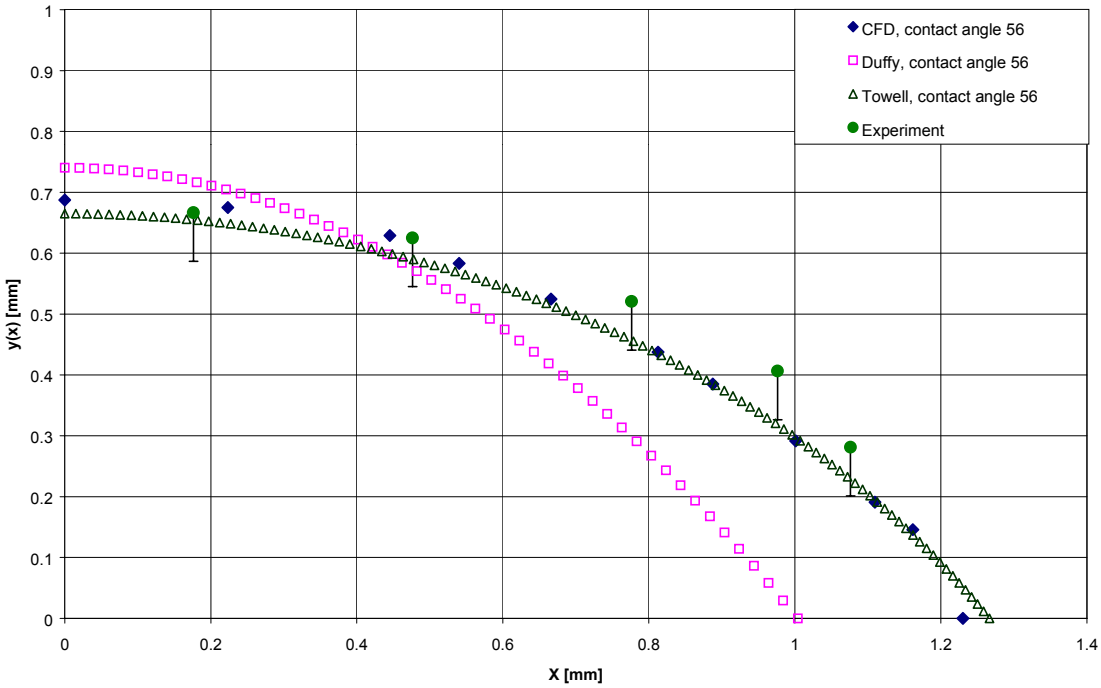

Fig. 8: Rivulet profiles from CFD simulation, experimental results and literature models [2, 11] (contact angle 56 degree, flow rate 15.77 ml/min, 298 K)

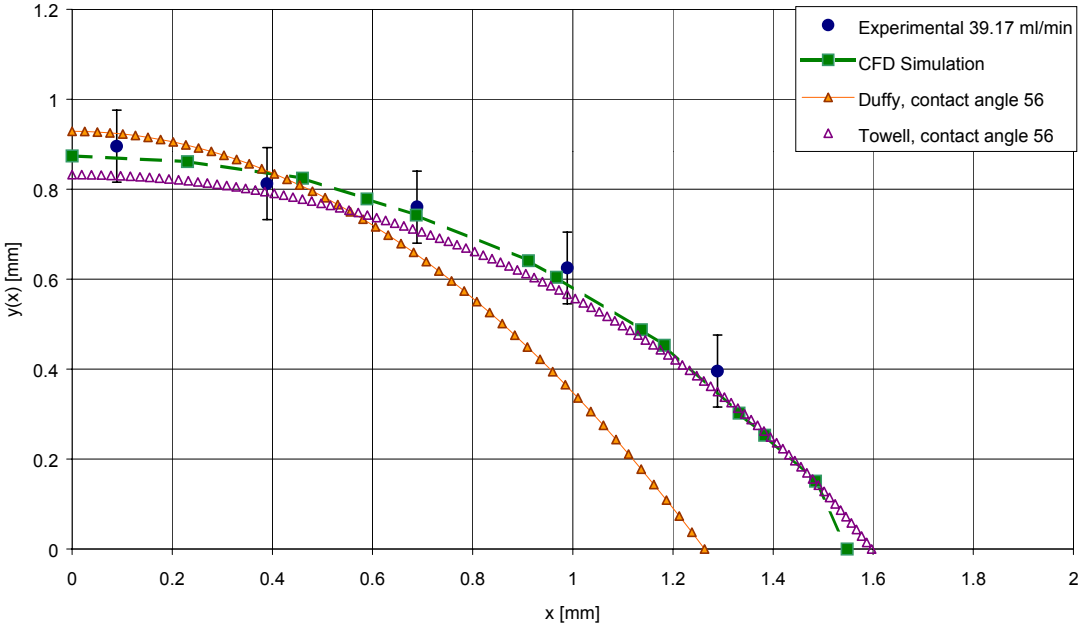

Fig. 9: Rivulet profiles from CFD simulation, experimental results and literature models [2, 11] (contact angle, 56 degree, flow rate 39.17 ml/min, 298 K)

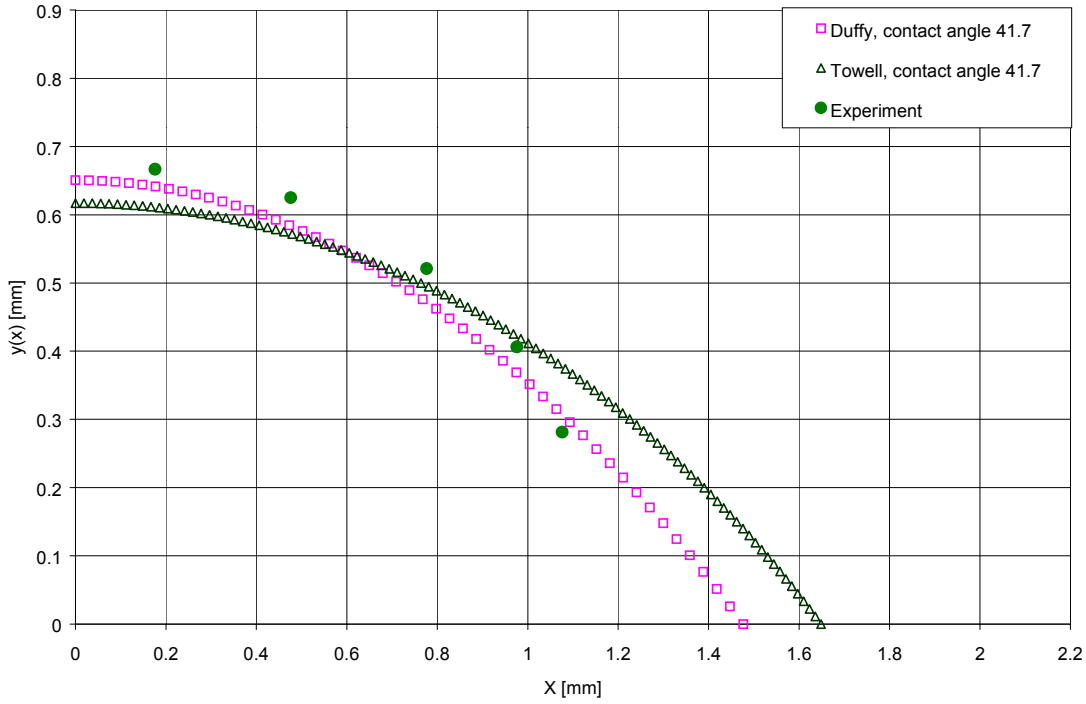

Fig. 10: Rivulet profiles from experimental results and literature models [2, 11] (contact angle 41.5 degree, flow rate 15.78 ml/min, 298 K)

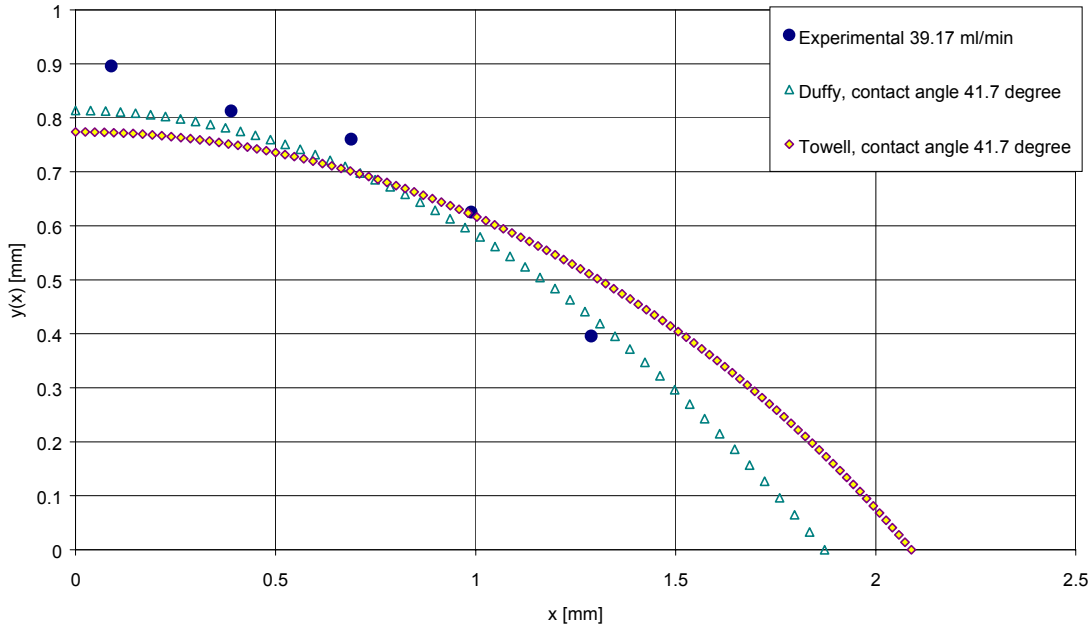

Fig. 11: Rivulet profiles from CFD simulation, experimental results and literature models [2, 11] (contact angle 41.5 degree, flow rate 15.78 ml/min, 298 K)

The maximum rivulet height reflects the interfacial effects. Fig. 12 shows the change of rivulet height with the flow rate. At low flow rates the maximum height increases more rapidly than at higher flow rates, which means a decrease in the interfacial effects. The CFD results and the Towell model are in good agreement with the experimental data when calculating using the static contact angle. The calculations were repeated again using the dynamic contact angle. An increase of the contact

angle from 41.7 to 56 have lead to an increase in the maximum rivulet height of about 12% for Duffy model and 7% for Towell model.

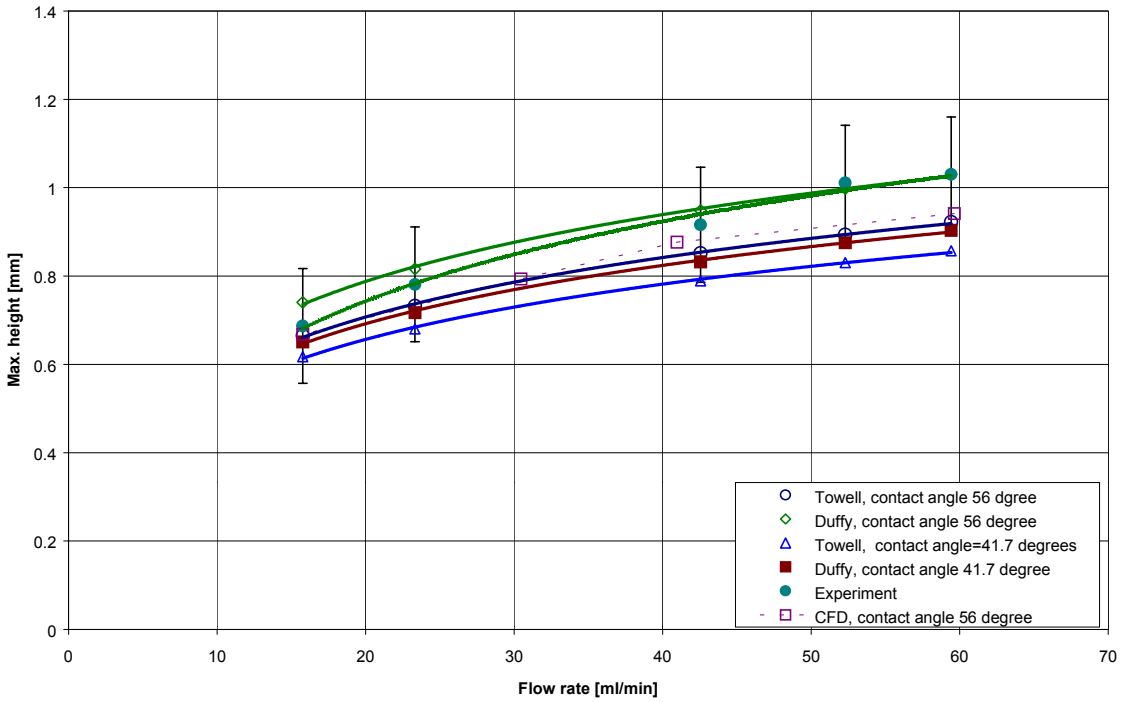

Fig. 12: Max. rivulet height as a function of the flow rate

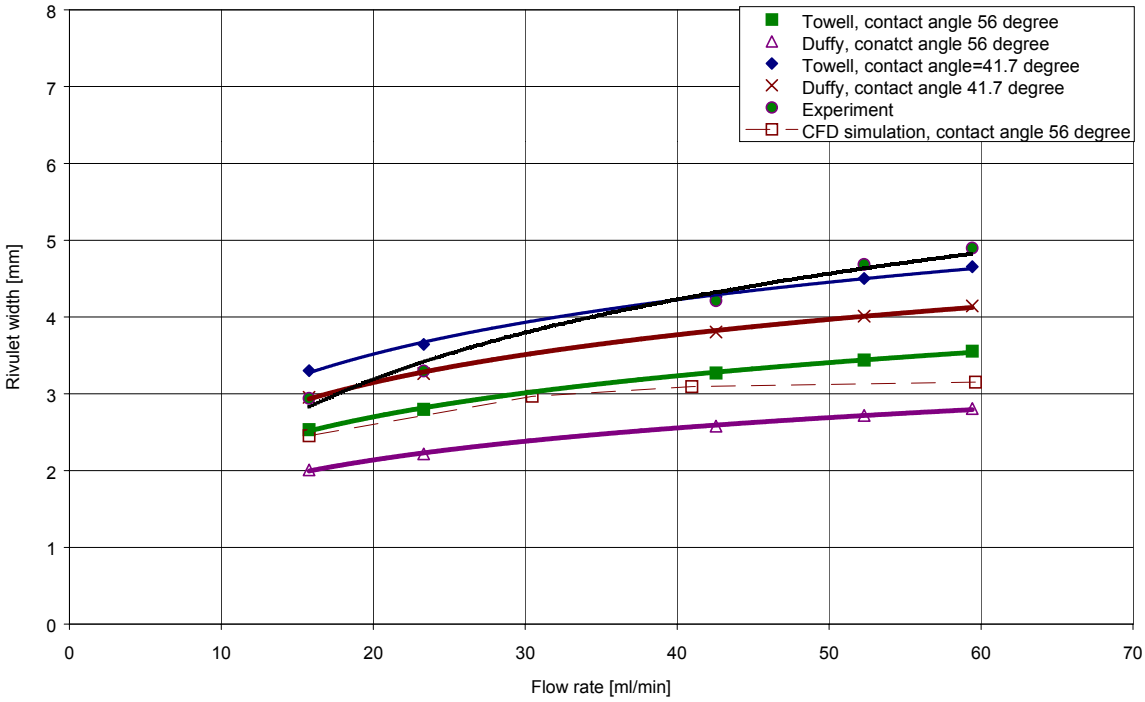

Fig. 13: Rivulet width as a function of flow rate.

The rivulet width as well as the contact angle could give an idea about the spreading of the liquid on a surface. Fig. 13 represents the rivulet width as a function of the flow rate. The calculations were performed for the two contact angles. For the dynamic contact angle Towell and Duffy model and for low flow rates agree with the experimental results more than for the higher flow rates. CFD simulation depending

on the static contact angle value gave values lower than the experimental ones. An increase of the contact angle from 41.7 to 56 have lead to an increase of about 30% in the rivulet width for Towell model and about 47% for Duffy model, which reflects the sensitivity of the flow to the contact angle.

Conclusions

In this paper a comparison between experimental results for the flow of a trickle on an inclined plate with CFD simulations and two analytical models were presented. A method to measure the spatial thickness of the rivulet were developed. This method is effective clean and cheap and did not need any additional materials or calibration and is applicable for all liquids. This method is also applicable when one has a wavy plate as is with a real distillation packing.

The static contact angle is a very important parameter and from the experimental results it seems to be constant and does not depend on the flow rate. However the measured static contact angle on a sample of the metal plate has given a value of 56 degree, the dynamic contact angle calculated using the curves in Figure (7) was 41.5. This difference resulted in the difficulties mentioned above in estimating the rivulet height near the rivulet edge. A better estimation of the contact angle would lead to more precise results.

The CFD simulation using the VOF model have given very good results so it can be used to simulate this kind of flow in a simple geometry in comparison to the experimental data and literature models. The work will be continued with other liquid mixtures and more complex geometries of structured metal packings, as is KÜHNI Rombopak®.

Literature

1. de Bruyn, J. R. (1992) Physical Reveiw A, 46, R4500-R4503.

2. Duffy, B. R. and Moffatt, H. L. (1995) The Chemical Engineering Journal, 60, 141-146.

3. Johnson, M. F. G., Bankoff, S. G. and Schulter, R. A. (1997) Rev. Sci. Instruments, 68, 4097-4102.

4. Johnson, M. F. G., Schulter, R. A. M., J., M. and Bankoff, S. G. (1999) J. Fluid Mech., 394, 339-354.

5. Kothe, D. B. R., W. J. (1995) Fluid Dynamics Group, Los Alamos National Laboratory. Report no. 65P05, 76T05, New Mexico.

6. Lechner, H. (2001) Krüss GmbH, (personal communication).

7. Leger, L. and Joanny, J. F. (1992) Rep. Prog. Phys., 55, 431-487.

8. Liu, J., Paul, J. D. and Gollub, J. P. (1993) J. Fluid Mech., 250, 69-101.

9. Shedd, T. A. N., T. A. (1998) Rev. of Sci. Instruments, 69, 4205-4213.

10. Szulczewska, B., Sek, J., Gorak, A. and Zbicinski, I. Paper at EFCE working party “Distillation, Absorption and Extraction”. Winterthur, Switzerland 3.-4.5.2000.

11. Towell, G. D. and Rothfeld, L. B. (1966) AIChE Journal, 12, 972-980.

12. Zhang, J. T. W., B. X.; Peng, X. F. (1999) Rev. Sci. Instruments, 71, 1883-1886.

13. FLUENT documentation (2001).